

# Detection of periodic variations in vertical velocities of Galactic masers

V. V. Bobylev<sup>1,2</sup> <sup>\*</sup> and A. T. Bajkova<sup>1</sup>

<sup>1</sup> Central (Pulkovo) Astronomical Observatory of RAS, 65/1 Pulkovskoye Chaussee, St. Petersburg, 196140, Russia

<sup>2</sup> Sobolev Astronomical Institute, St. Petersburg State University, Bibliotchnaya pl. 2, St. Petersburg, 198504, Russia

Accepted 2014 MONTH XX.

## ABSTRACT

We have collected literature data on Galactic masers with trigonometric parallaxes measured by means of VLBI. We have obtained series of residual tangential,  $\Delta V_{\text{circ}}$ , and radial,  $\Delta V_R$ , velocities for 107 masers. Based on these series, we have re-determined parameters of the Galactic spiral density wave using the method of spectral (periodogram) analysis. The tangential and radial perturbation amplitudes are  $f_\theta = 6.0 \pm 2.6 \text{ km s}^{-1}$  and  $f_R = 7.2 \pm 2.2 \text{ km s}^{-1}$ , respectively; the perturbation wavelengths are  $\lambda_\theta = 3.2 \pm 0.5 \text{ kpc}$  and  $\lambda_R = 3.0 \pm 0.6 \text{ kpc}$  for a four-armed spiral model,  $m = 4$ . The phase of the Sun  $\chi_\odot$  in the spiral density wave is  $-79^\circ \pm 14^\circ$  and  $-199^\circ \pm 16^\circ$  from the residual tangential and radial velocities, respectively. The most interesting result of this work is detecting a wave in vertical spatial velocities ( $W$ ) versus distance  $R$  from the Galactic rotation axis. From the spectral analysis, we have found the following characteristics of this wave: the perturbation wavelength is  $\lambda_W = 3.4 \pm 0.7 \text{ kpc}$  and the amplitude  $f_W = 4.3 \pm 1.2 \text{ km s}^{-1}$ .

**Key words:** Masers – SFRs – Spiral Arms: Galaxy (Milky Way).

## 1 INTRODUCTION

Like many other galaxies, our Galaxy is characterized by a spiral structure. There exist numerous models explaining the origin and maintenance of the spiral pattern. Proposed models include the swing amplification of noise (Goldreich & Lynden-Bell 1965; Julian & Toomre 1966), groove modes (Sellwood & Lin 1989; Sellwood & Kahn 1991; Sellwood 2012) or other modes (Lin & Shu 1964), possibly recurrent (Sellwood & Carlberg 2014).

Most models of the Galaxy's spiral structure consider only perturbations of radial and tangential velocities in the Galactic plane. It is interesting to note that large-scale, coherent vertical motions have been found in the disc of the Milky Way in SEGUE (Widrow et al. 2012), RAVE (Williams et al. 2013) and LAMOST (Carlin et al. 2013) data.

Non-zero vertical velocities of objects are usually explained with impact of external objects, like dwarf galaxies (companions) or clouds of dark matter, crossing the Galactic disk. However, it is possible to explain them without involvement of any external forces. In the framework of the theory of spiral density waves, small fluctuations can occur in the direction perpendicular to the Galactic plane. For example, Fridman (2007) pointed out the possibility of such

fluctuations. Numerical simulations made recently by various authors (for example, Faure et al. (2014) and Debattista (2014)) showed that the spiral density wave in the Galaxy might lead to the emergence of vertical fluctuations with an average amplitude of 10–20  $\text{km s}^{-1}$ .

Galactic masers with known trigonometric parallaxes measured by means of VLBI (Reid et al. 2009; Honma et al. 2012; Reid et al. 2014) give unprecedented opportunity to study fine kinematical effects. Relative measurement errors of parallaxes provided by VLBI are, on average, less than 10%. Currently, the number of such objects is already 119. In this Letter, we re-determine parameters of the Galactic spiral density wave from radial and tangential velocities of these 119 masers and investigate their vertical velocities for periodicities which can be associated with the influence of the Galactic spiral density wave.

## 2 METHOD

From observations, we have heliocentric line-of-sight velocity  $V_r$  in  $\text{km s}^{-1}$ ; proper-motion velocity components  $V_l = 4.74r\mu_l \cos b$  and  $V_b = 4.74r\mu_b$ , in the  $l$  and  $b$  directions respectively (the coefficient 4.74 is the number of kilometers in an astronomical unit divided by the number of seconds in a tropical year); heliocentric distance  $r$  in kpc for a star. The proper motion components  $\mu_l \cos b$  and  $\mu_b$  are measured in

\* E-mail: vbobylev@gao.spb.ru

mas yr<sup>-1</sup>. We adopt  $R_0 = 8.0 \pm 0.4$  kpc for the galactocentric distance of the Sun.

The components  $U, V, W$  of stellar spatial velocities are determined from the observed line-of-sight and tangential velocities in the following way:

$$\begin{aligned} U &= V_r \cos l \cos b - V_l \sin l - V_b \cos l \sin b, \\ V &= V_r \sin l \cos b + V_l \cos l - V_b \sin l \sin b, \\ W &= V_r \sin b + V_b \cos b. \end{aligned} \quad (1)$$

Velocity  $U$  is directed towards the Galactic center;  $V$ , along the Galactic rotation; and  $W$ , towards the Northern Galactic pole.

Two projections of these velocities:  $V_R$ , directed radially from the Galactic center towards an object, and  $V_{circ}$ , orthogonal to  $V_R$  and directed towards Galactic rotation, are found from the following relations:

$$\begin{aligned} V_{circ} &= U \sin \theta + (V_0 + V) \cos \theta, \\ V_R &= -U \cos \theta + (V_0 + V) \sin \theta, \end{aligned} \quad (2)$$

where  $V_0 = |R_0 \Omega_0|$ , and the position angle  $\theta$  is determined as  $\tan \theta = y/(R_0 - x)$ , where  $x, y$  are Galactic Cartesian coordinates of an object. The quantity  $\Omega_0$  is the Galactic angular rotational velocity at distance  $R_0$ ; parameters  $\Omega_0^1, \dots, \Omega_0^n$  are derivatives of the angular velocity from the first to the  $n$ th order, respectively.

Velocities  $V_R$  are practically independent and velocities  $W$ , independent from the nature of the Galactic rotation curve. However, to analyze periodicities in the tangential velocities, it is necessary to find parameters of a smooth rotation curve and to form residual velocities  $\Delta V_{circ}$ . As it is shown by practice, to build a smooth rotation curve in a wide range of distances  $R$ , it is sufficient to have values of two derivatives of the Galactic rotation angular velocity:  $\Omega_0'$  and  $\Omega_0''$ . All the three velocities:  $V_R, \Delta V_{circ}$  and  $W$  must be corrected for the solar peculiar velocity  $U_\odot, V_\odot, W_\odot$ .

To determine the angular rotational velocity  $\Omega_0$  and its two derivatives,  $\Omega_0'$  and  $\Omega_0''$ , from observational data, we use the equations derived from Bottlinger's formulas with the angular velocity of Galactic rotation  $\Omega$  expanded in a series to terms of the second order of smallness in  $r/R_0$ :

$$\begin{aligned} V_r &= -U_\odot \cos b \cos l - V_\odot \cos b \sin l - W_\odot \sin b \\ &+ R_0(R - R_0) \sin l \cos b \Omega_0' \\ &+ 0.5 R_0(R - R_0)^2 \sin l \cos b \Omega_0'', \end{aligned} \quad (3)$$

$$\begin{aligned} V_l &= U_\odot \sin l - V_\odot \cos l - r \Omega_0 \cos b \\ &+ (R - R_0)(R_0 \cos l - r \cos b) \Omega_0' \\ &+ 0.5(R - R_0)^2 (R_0 \cos l - r \cos b) \Omega_0'', \end{aligned} \quad (4)$$

$$\begin{aligned} V_b &= U_\odot \cos l \sin b + V_\odot \sin l \sin b - W_\odot \cos b \\ &- R_0(R - R_0) \sin l \sin b \Omega_0' \\ &- 0.5 R_0(R - R_0)^2 \sin l \sin b \Omega_0'', \end{aligned} \quad (5)$$

where the distance  $R$  of an object from the Galactic rotation axis is expressed as

$$R^2 = r^2 \cos^2 b - 2R_0 r \cos b \cos l + R_0^2. \quad (6)$$

According to the linear theory of density waves (Lin & Shu 1964),

$$\begin{aligned} V_R &= -f_R \cos \chi, \\ \Delta V_{circ} &= f_\theta \sin \chi, \end{aligned} \quad (7)$$

where

$$\chi = m[\cot(i) \ln(R/R_0) - \theta] + \chi_\odot \quad (8)$$

is the phase of the spiral wave ( $m$  is the number of spiral arms;  $i$  is the pitch angle;  $\chi_\odot$  is the radial phase of the Sun in the spiral wave;  $f_R$  and  $f_\theta$  are amplitudes of radial and tangential components of the perturbed velocities which, for convenience, are always considered positive).

First, we use Bottlinger's equations (3)–(5) only for construction of the Galactic rotation curve. Deviations of tangential velocities from this curve give residual tangential velocities  $\Delta V_{circ}$ . It is possible, however, to obtain a solution for amplitudes of radial and tangential perturbations, wavelength and phase of the Sun including (7) into Bottlinger's equations as shown by Mishurov et al. (1979). Because the vertical velocities  $W$  of interest are not included to the model, we next decided to use spectral analysis as unified approach to study periodicities in all velocity sets:  $V_R, \Delta V_{circ}$  and  $W$  separately. Note that if radial and residual tangential velocities correspond to the Lin& Shu model (7), then separate and joint solutions should be the same. If results differ, we can assume that there is some discrepancy between data and the model (7). Below we will compare separate and joint solutions, obtained from the  $V_R$  and  $\Delta V_{circ}$  sets.

We use the effective method of spectral (periodogram) analysis based on Fourier transform, modified for analysis of logarithmic spirals and accounting for position angles of the analyzed objects (Bajkova & Bobylev 2012).

The parameter  $\lambda$ , the distance (along the Galactocentric radial direction) between adjacent spiral arm segments in the Solar neighborhood (the wavelength of the spiral density wave), is calculated from the relation:

$$\frac{2\pi R_0}{\lambda} = m \cot(i). \quad (9)$$

Let there be a series of measured velocities  $V_n(R_n)$  (these can be both radial,  $V_R$ , and residual tangential,  $\Delta V_\theta$ , velocities) at points with Galactocentric distances  $R_n$  and position angles  $\theta_n$ ,  $n = 1, \dots, N$  where  $N$  is the number of objects. The objective of our spectral analysis is to extract a periodicity from the data series in accordance with the model describing a spiral density wave with parameters  $f_R$  ( $f_\theta$ ),  $\lambda(i)$  and  $\chi_\odot$ .

Having taken into account the logarithmic character of the spiral density wave and the position angles of the objects  $\theta_n$ , our spectral (periodogram) analysis of the series of velocity perturbations is reduced to calculating the square of the amplitude (power spectrum) of the standard Fourier transform: (Bajkova & Bobylev 2012):

$$\bar{V}_{\lambda_k} = \frac{1}{N} \sum_{n=1}^N V_n'(R_n') \exp\left(-j \frac{2\pi R_n'}{\lambda_k}\right), \quad (10)$$

where  $\bar{V}_{\lambda_k}$  is the  $k$ th harmonic of the Fourier transform, with the wavelength  $\lambda_k = D/k$ ;  $D$  is the period of the series being analyzed,

$$\begin{aligned} R_n' &= R_0 \ln(R_n/R_0), \\ V_n'(R_n') &= V_n(R_n) \times \exp(jm\theta_n). \end{aligned} \quad (11)$$

The algorithm of searching for periodicities modified to properly determine not only the wavelength but also the amplitude of the perturbations is described in detail in Bajkova & Bobylev (2012).

Obviously, the sought-for wavelength  $\lambda$  corresponds to the peak value of the power spectrum  $S_{peak}$ . The pitch angle of the spiral density wave can be derived from Eq. (9). We determine the perturbation amplitude and phase by fitting the harmonic with the wavelength found to the observational data. The following relation can also be used to estimate the perturbation amplitude:

$$f_R(f_\theta) = \sqrt{4 \times S_{peak}}.$$

### 3 DATA

We use coordinates and trigonometric parallaxes of masers measured by VLBI with errors that are, on average, below 10%. These masers are related to very young objects (basically protostars of high masses, but there are also those with low masses; a number of massive supergiants are known as well) located in active star-forming regions.

One of such observational campaigns is the Japanese project VERA (VLBI Exploration of Radio Astrometry) for observations of water (H<sub>2</sub>O) Galactic masers at 22 GHz (Hirota et al. 2007) and SiO masers (such masers are very rare among young objects) at 43 GHz (Kim et al. 2008).

Water and methanol (CH<sub>3</sub>OH) maser parallaxes are observed in the USA (VLBA) at 22 GHz and 12 GHz (Reid et al. 2009). Methanol masers are observed also in the framework of the European VLBI network (Rygl et al. 2010). These two projects are combined in the BeSSeL program (Brunthaler et al. 2011).

VLBI observations of radio stars in continuum at 8.4 GHz (Torres et al. 2007; Dzib et al. 2011) are carried out with the same goals. In the framework of this program, low-mass nearby stars closely associated with the Gould belt are observed.

Reid et al. (2014) present a summary of measurements of trigonometric parallaxes, proper motions and radial velocities of 103 masers. To this sample, six more sources in the Local arm were added from the list in Xu et al. (2013): EC 95, L 1448C, S1, DoAr21, SVC13/NGC1333, IRAS 16293–2422; then, we add two red supergiants, PZ Cas (Kusuno et al. 2013) and IRAS 22480+6002 (Imai et al. 2012), and finally, IRAS 22555+6213 (Chibueze et al. 2014), Cyg X-1 (Reid et al. 2011), IRAS 20143+3634 (Burns et al. 2014), and five low-mass close radio stars in Taurus: Hubble 4 and HDE 283572 (Torres et al. 2007), T Tau N (Loinard et al. 2007), HP Tau/G2 (Torres et al. 2009) and V773 Tau (Torres et al. 2012). Thus, the whole sample contains 119 sources.

### 4 RESULTS AND DISCUSSION

We found the following components of the Solar peculiar velocity and Galactic rotation parameters:

$$\begin{aligned} (U_\odot, V_\odot, W_\odot) &= (6.8, 15.9, 8.3) \pm (1.2, 1.2, 0.9) \text{ km s}^{-1} \\ \Omega_0 &= 29.53 \pm 0.49 \text{ km s}^{-1} \text{ kpc}^{-1}, \\ \Omega'_0 &= -4.27 \pm 0.10 \text{ km s}^{-1} \text{ kpc}^{-2}, \\ \Omega''_0 &= 0.874 \pm 0.050 \text{ km s}^{-1} \text{ kpc}^{-3}. \end{aligned} \quad (12)$$

This solution has been obtained by least squares using 107 masers. Following the recommendation of Reid et al. (2014),

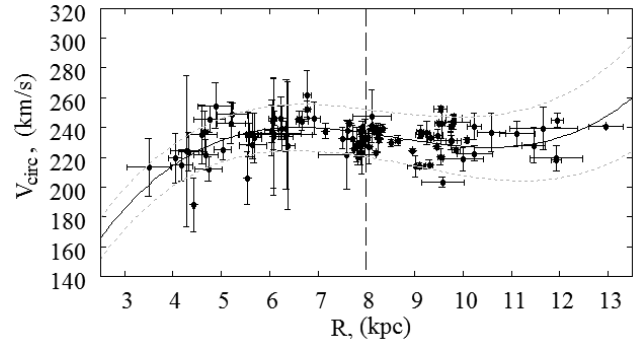


**Figure 1.** The rotation curve of the Galaxy, built with the parameters (12). The vertical line indicates the position of the Sun. The borders of  $1\sigma$  confidence intervals correspond to the  $\sigma_{R_\odot} = 0.4$  kpc errors and errors of Galactic rotation parameters (12).

when determining the Galaxy rotation parameters, masers located at distances  $R < 4$  kpc were excluded because of the influence of the Central Galactic bar at these distances. Then, several additional sources were excluded on the base of the  $3\sigma$  criterion: G09.62+0.19, G10.62–0.38, G12.02–0.03, G23.70–0.19, G25.70+0.04, G27.36–0.16, G78.12+3.63, G168.06+0.82 and G182.67–3.26. In addition, we did not use the maser G28.86+0.06 that has a too high velocity,  $W > 50$  km/s.

The Galaxy rotation curve, built with the parameters (12), is presented in Fig. 1. Next, we rejected 12 masers belonging to the Gould belt in order to avoid the influence of its peculiar properties on the results of further analysis. Velocities  $V_R$ ,  $\Delta V_{circ}$  and  $W$  of 95 masers versus  $R$  are shown in Fig. 2. In this figure, a periodicity in  $V_R$  perturbations is clearly visible. Such fluctuations are associated with the Galactic spiral density wave. Earlier, we managed to estimate the spiral density wave parameters quite reliably from a lower number of masers (Bobylev & Bajkova 2010, 2013). Surprisingly, periodic perturbations in  $W$  velocities are visible in Fig. 2 even by eye. In Fig. 3, power spectra of the radial  $V_R$ , residual tangential  $\Delta V_{circ}$  and vertical  $W$  velocities of masers are displayed. For application of the spectral analysis described above, we adopt a four-armed spiral model (Bobylev & Bajkova 2014a),  $m = 4$ . The tangential and radial perturbation amplitudes we obtained are  $f_\theta = 6.0 \pm 2.6 \text{ km s}^{-1}$  and  $f_R = 7.2 \pm 2.2 \text{ km s}^{-1}$ , respectively. The perturbation wavelengths are  $\lambda_\theta = 3.2 \pm 0.5 \text{ kpc}$  and  $\lambda_R = 3.0 \pm 0.6 \text{ kpc}$ . Note that all the error bars were found using the Monte-Carlo statistical method. Significance levels of all the spectrum peaks shown in Fig. 3 are not lower than 0.995.

Based on our estimates of the wavelength  $\lambda$ , we found the pitch angle for the four-armed spiral pattern ( $m = 4$ ) from equation (9) for each component of the velocity independently:  $i_R = -13.4^\circ \pm 2.7^\circ$ ,  $i_\theta = -14.3^\circ \pm 2.3^\circ$ . These two values are in a good agreement with the estimate  $i = -13 \pm 1^\circ$  for  $m = 4$ , obtained earlier using spatial distribution of 73 masers (Bobylev & Bajkova 2014a).

The most interesting result of this study is detection of a periodic wave in vertical  $W$  velocities versus distance  $R$  which is especially noticeable in the area of the Local arm and Perseus arm ( $R \approx 9.5$  kpc). From our spectral

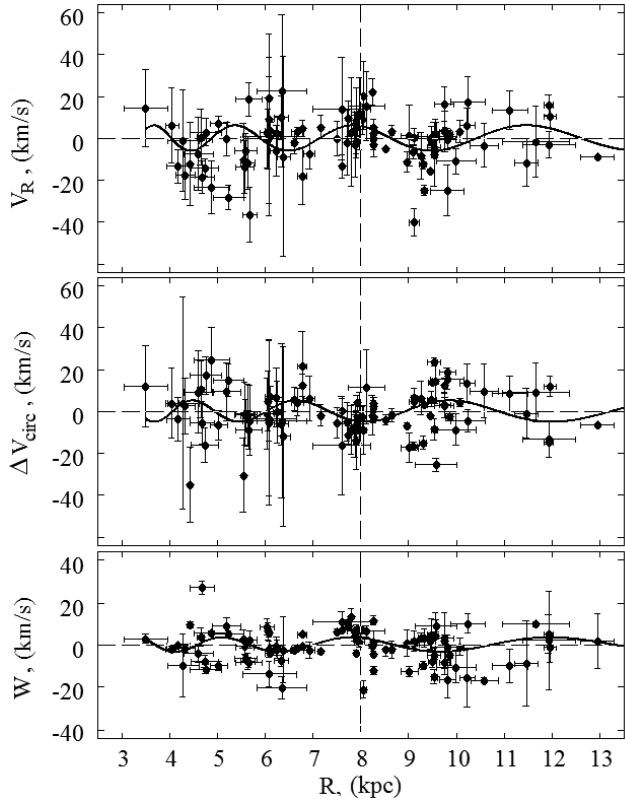


**Figure 2.** The radial  $V_R$ , residual tangential  $\Delta V_{circ}$  and vertical velocities  $W$  of masers versus distances  $R$ . The vertical dashed line indicates the position of the Sun.

analysis, we found the following characteristics of this wave: the perturbation wavelength is  $\lambda = 3.4 \pm 0.7$  kpc and the amplitude,  $f_W = 4.3 \pm 1.2$  km s<sup>-1</sup>.

The waves found for all three velocity sets are shown in Fig. 2 (solid curves). The logarithmic nature of the waves is clearly visible. Directly at the distance of the Sun, the top of the radial velocity wave has a displacement in the direction to the Galaxy center by  $+19^\circ$ ; the shift of the tangential velocities wave is  $-11^\circ$  and that of the vertical velocities  $W$  wave is  $+21^\circ$ . Usually we count the phase of the Sun from the Carina–Sagittarius arm ( $R \approx 6.5$  kpc) according to Rohlfs (1977). In this case, for the radial velocities we have  $(\chi_\odot)_R = -199^\circ \pm 16^\circ$  and for the tangential velocities,  $(\chi_\odot)_\theta = -79^\circ \pm 14^\circ$ .

Note that the wave found in the tangential velocities contradicts the simple theory (Lin & Shu 1964), as in the center of arms (for example, the Carina–Sagittarius arm) these velocities should be equal to zero. So we have a discrepancy with the theory amounting to  $\pi/2$ . On the other hand, the obtained values of the phase of the Sun are in a good agreement with the values found from data on 73 masers in Bobylev & Bajkova (2013),  $-50^\circ \pm 15^\circ$  and  $-160^\circ \pm 15^\circ$  from the residual tangential and radial velocities, respectively.

Now we present results of our solution of the Bottlinger’s equations which include perturbations from the spiral density wave (7) in accordance with the linear Lin& Shu theory (Mishurov et al. 1979), where amplitudes of radial and tangential perturbations, pitch angle and phase of the Sun are free parameters. The results are the following: the

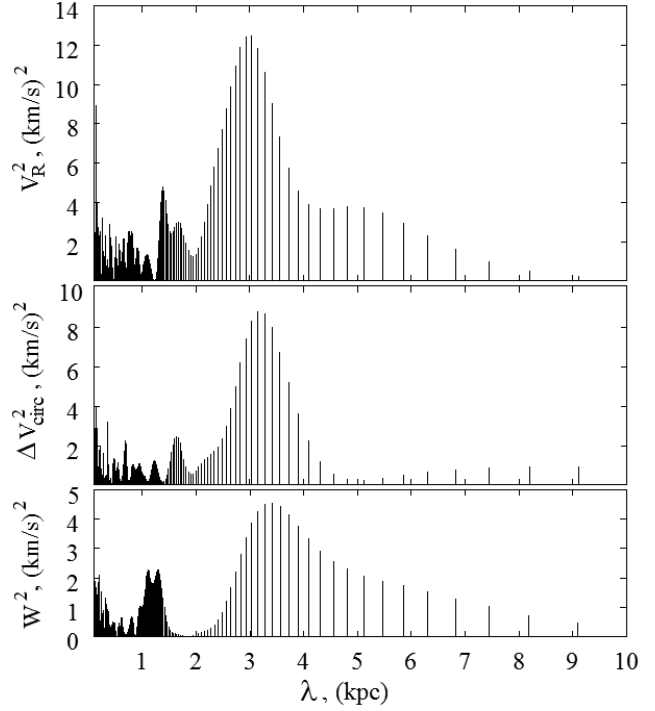


**Figure 3.** Power spectra of the radial  $V_R$ , residual tangential  $\Delta V_{circ}$  and vertical  $W$  velocities of masers.

amplitude of radial perturbations is  $f_R = 6.0 \pm 1.4$  km s<sup>-1</sup>; that of tangential perturbations,  $f_\theta = 0.6 \pm 2.3$  km s<sup>-1</sup>; the pitch angle is  $i = -11.7^\circ \pm 4.9^\circ$  for the four-armed spiral model,  $m = 4$ ; the phase of the Sun is  $\chi_\odot = -118^\circ \pm 22^\circ$ . We see that the amplitude of tangential perturbations is not significant, although oscillations are clearly seen in the data (Fig. 2). This result differs from that obtained using spectral analysis, which can be explained by a discrepancy between the data and Lin& Shu model.

For the perturbations of vertical velocities  $W$ , there exists no theory, but as it can be seen from Fig. 2, the wave in  $W$  velocities is similar to the wave in radial velocities. Such a result is in quite a good agreement with the results of numerical simulations (Faure et al. 2014; Debattista 2014).

As follows from the simulation results (Faure et al. 2014; Debattista 2014), the vertical velocities can be inverted depending on the hemisphere. We checked this effect on our sample of masers, though it is not so large. We divided the whole sample in half — into the North and South parts, and got two solutions:  $(f_W)_{North} = 3.9 \pm 2.0$  km s<sup>-1</sup>,  $\lambda_{North} = 3.5 \pm 1.1$  kpc and  $(f_W)_{South} = 4.4 \pm 2.0$  km s<sup>-1</sup>,  $\lambda_{South} = 3.5 \pm 1.2$  kpc. Thus, we can see that these solutions for amplitudes and wavelengths differ slightly from those found using the whole data set. The phase shift between the Northern and Southern waves is only about 20 degrees. We conclude that the inversion is not detected. In Fig. 4, vertical velocities, together with the fitted waves (solid curves), are shown for the galactic North and South hemispheres.

## 5 CONCLUSIONS

We have collected literature data on 119 Galactic masers with known trigonometric parallaxes measured by means

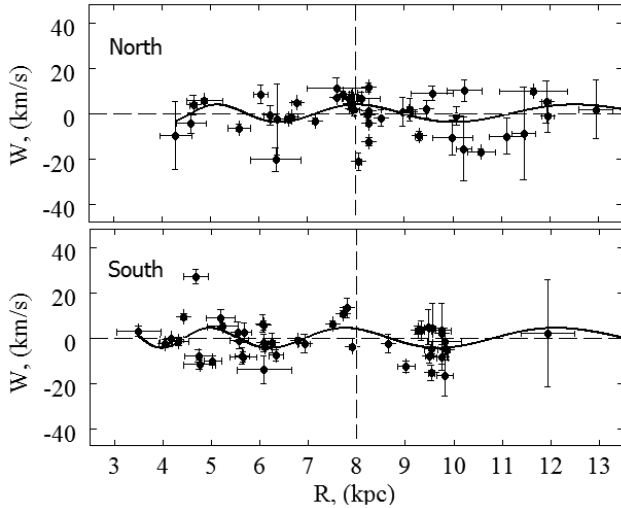


**Figure 4.** The vertical  $W$  velocities of masers versus  $R$ . The vertical dashed line indicates the position of the Sun.

of VLBI. Based on these series, we have re-determined the parameters of the Galactic spiral density wave using the method of periodogram analysis.

We rejected 12 masers belonging to the Gould belt in order to avoid the influence of its peculiar properties on the results of the further analysis. The tangential and radial perturbation amplitudes are  $f_\theta = 6.0 \pm 2.6 \text{ km s}^{-1}$  and  $f_R = 7.2 \pm 2.6 \text{ km s}^{-1}$ , respectively; the perturbation wavelength is  $\lambda_\theta = 3.2 \pm 0.5 \text{ kpc}$  and  $\lambda_R = 3.0 \pm 0.6 \text{ kpc}$ . Based on the derived values of  $\lambda$ , a new value of the kinematic pitch angle for a four-armed spiral pattern is obtained:  $i = -13.9 \pm 2.5^\circ$ . The phase of the Sun  $\chi_\odot$  in the spiral density wave is  $-79^\circ \pm 14^\circ$  and  $-199^\circ \pm 16^\circ$  from the residual tangential and radial velocities, respectively (we measured the phase from the Carina–Sagittarius arm).

The most interesting result of this work is detecting a wave in the  $W$  spatial velocities versus distance  $R$  which is especially noticeable in the area of the Local arm and the Perseus arm. From our spectral analysis, we have found the following characteristics of this wave: the perturbation wavelength is  $\lambda_W = 3.4 \pm 0.7 \text{ kpc}$  and the amplitude,  $f_W = 4.3 \pm 1.2 \text{ km s}^{-1}$ . The wave obtained from  $W$  velocities is closer to the wave obtained from radial velocities. We found that similar wave parameters can be derived both from the Northern and Southern masers.

## ACKNOWLEDGEMENTS

The authors are thankful to the anonymous referee for critical remarks which permitted to improve the paper. This study was supported by the “Nonstationary Phenomena in Objects of the Universe” Program of the Presidium of Russian Academy of Sciences (P–21). The authors are thankful to Nikolai Samus’ for editing the text.

## REFERENCES

Bajkova A.T., Bobylev V.V., 2012, *Astron. Lett.* 38, 549  
 Bobylev V.V., Bajkova A.T., 2010, *MNRAS* 408, 1788

Bobylev V.V., Bajkova A.T., 2013, *Astron. Lett.*, 39, 809  
 Bobylev V.V., Bajkova A.T., 2014a, *MNRAS* 437, 1549  
 Bobylev V.V., Bajkova A.T., 2014a, *MNRAS* 441, 142  
 Burns R.A., Yamaguchi Y., Handa T., et al., 2014, arXiv:1404.5506  
 Brunthaler A., Reid M.J., Menten K.M., et al., 2011, *AN* 332, 461  
 Carlin J.L., DeLaunay J., Newberget H.J., et al., 2013, *ApJ*, 777, L5  
 Chibueze J.O., Sakanoue H., Nagayama T., et al., 2014, arXiv:1406.277  
 Debattista V., 2014, *MNRAS*, 443, L1  
 Dzib S., Loinard L., Rodriguez L.F., et al., 2011, *ApJ* 733, 71  
 Faure C., Siebert A., Famaey B., 2014, *MNRAS* 440, 2564  
 Fridman A.M., 2007, *Physics Uspekhi* 50, 115  
 Goldreich, P., Lynden-Bell D., 1965, *MNRAS*, 130, 125  
 Julian W. H., Toomre A., 1966, *ApJ*, 146, 810  
 Honma M., Nagayama T., Ando K., et al., 2012, *PASJ* 64, 136  
 Hirota T., Bushimata T., Choi Y.K., et al., 2007, *PASJ* 59, 897  
 Imai H., Sakai N., Nakanishi H., et al., 2012, *PASJ* 64, 142  
 Kim M.K., Hirota T., Honma M., et al., 2008, *PASJ* 60, 991  
 Kusuno K., Asaki Y., Imai H., and Oyama T., 2013, *ApJ* 774, 107  
 Lin C.C., Shu F.H., 1964, *ApJ* 140, 646  
 Loinard L., Torres R.M., Mioduszewski A.J., et al., 2007, *ApJ* 671, 546  
 Mishurov Yu.N., Pavlovskaya E.D., Suchkov A.A., 1979, *Sov. Astron.* 23, 147  
 Reid M.J., Menten K.M., Zheng X.W., et al., 2009, *ApJ* 700, 137  
 Reid M.J., McClintock J.E., Narayan R., et al., 2011, *ApJ* 742, 83  
 Reid M.J., Menten K.M., Zheng X.W., et al., 2014, *ApJ* 783, 130  
 Rohlfs K., *Lectures on density wave theory. Lecture Notes in Physics*, Berlin: Springer Verlag, 1977  
 Rygl K.L.J., Brunthaler A., Reid M.J., et al., 2010, *A&A* 511, A2  
 Sellwood J.A., 2012, *ApJ*, 751, 44  
 Sellwood J.A., Carlberg R.G., 2014, *ApJ*, 785, 137  
 Sellwood J.A., Kahn F.D., 1991, *MNRAS*, 250, 278  
 Sellwood J.A., Lin D.N.C., 1989, *MNRAS*, 240, 991  
 Torres R.M., Loinard L., Mioduszewski A.J., et al., 2007, *ApJ* 671, 1813  
 Torres R.M., Loinard L., Mioduszewski A.J., et al., 2009, *ApJ* 698, 242  
 Torres R.M., Loinard L., Mioduszewski A.J., et al., 2012, *ApJ* 747, 18  
 Widrow L.M., Gardner S., Yanny, B., et al., 2012, *ApJ* 750, L41  
 Williams M.E.K., Steinmetz M., Binney J., et al., 2013, *MNRAS*, 436, 101  
 Xu Y., Li J.J., Reid M.J., et al., 2013, *ApJ* 769, 15